JLB

Article

Reduction of indoxyl sulfate by AST-120 attenuates monocyte inflammation related to chronic kidney disease

Shunsuke Ito,[*,†] Yusuke Higuchi,[†] Yoko Yagi,[†] Fuyuhiko Nishijima,[†] Hideyuki Yamato,[†] Hideto Ishii,[*] Mizuko Osaka,[*] and Masayuki Yoshida*[*,1]*

*Life Science and Bioethics, Department of International Health Development, Tokyo Medical and Dental University, Tokyo, Japan; and †Biomedical Research Laboratories, Kureha Corporation, Tokyo, Japan

RECEIVED JANUARY 19, 2012; REVISED DECEMBER 18, 2012; ACCEPTED DECEMBER 31, 2012. DOI: 10.1189/jlb.0112023

ABSTRACT

Accelerated cardiovascular disease is a frequent complication of CKD. Monocyte-mediated inflammation and adhesion of monocytes to vascular endothelium are key events in atherogenesis. An oral adsorbent, AST-120, retards renal function deterioration by lowering IS, which is known to accumulate in CKD patients. However, the effect of AST-120 on CKD-related monocyte activation is unknown. We aimed to determine whether AST-120 improves monocyte-mediated inflammation through IS reduction. Flow cytometric analysis showed that Mac-1 expression and ROS production were significantly higher in peripheral blood monocytes of subtotal Nx CKD mice than in sham-operated mice. AST-120 treatment significantly decreased Mac-1 expression and ROS production in CKD model mice. Furthermore, administration of IS induced monocyte-mediated inflammation and ROS generation. In vitro studies indicated that IS dose-dependently increased THP-1 monocytic cell adhesion to IL-1β-activated HUVECs under physiological flow conditions. IS also induced monocyte-mediated inflammation and ROS production in THP-1 cells. Phosphorylation of p38 MAPK and membrane translocation of NAD(P)H oxidase subunit p47phox in THP-1 cells were induced by IS. Both SB203580 (p38 MAPK inhibitor) and apocynin [NAD(P)H oxidase inhibitor] reduced THP-1 cell adhesion to HUVECs. Apocynin also inhibited IS-induced ROS production in THP-1 cells. IS induced monocyte-driven inflammation through NAD(P)H oxidase- and p38 MAPK-dependent pathways in monocytes. The main finding of this study was that AST-120 inhibited monocyte activation by reducing IS in vivo. This provides new insights on how AST-120 attenuates the progression of atherosclerosis in CKD.

***J. Leukoc. Biol.* 93: 837–845; 2013.**

Introduction

Cardiovascular disease is a major cause of death in CKD [1]. Atherosclerosis is highly prevalent in patients with severe renal failure, and it advances more rapidly in individuals with renal dysfunction than in healthy individuals [2]. Reduced kidney function is associated with the risk of developing cardiovascular disease, even when the dysfunction is mild [3]. In recent years, the relationship between cardiovascular dysfunction and renal insufficiency has been referred to as the "cardiorenal syndrome". Many factors, such as development of uremic toxin, chronic inflammation, anemia, malnutrition, and renin angiotensin aldosterone system, are considered to affect the cardiovascular system and kidney function [4].

Monocyte recruitment to the vascular endothelium plays an important role in the development of atherosclerosis [5] and may occur through a variety of selectin- and integrin-dependent mechanisms [6]. Leukocyte adhesion to the inflamed endothelium involves the β2-integrin family of receptors (which share a common β2 subunit), such as LFA-1 (CD11a/CD18), Mac-1 (CD11b/CD18), p150,95/CR4 (CD11c/CD18), and CD11d/CD18 [7–9]. Mac-1 is a receptor for ICAM-1 and ECMs, which are abundant in injured tissue. Mac-1 inactivation (by a mAb) or depletion (by gene targeting) prevents neointima formation after vascular injury [10, 11], suggesting a dominant role for Mac-1 in development of atherosclerosis. Oxidative stress is also a major cause of cardiovascular disease and other complications of renal disease [12]. Oxidative stress can provoke inflammation by generating proinflammatory cytokines and chemokines [13, 14], which are capable of inducing oxidative stress and mediating Mac-1 expression on the cell surface of monocytes [15]. Recently, Mac-1 overexpression and increased ROS generation has been observed in patients with end-stage renal disease [12], suggesting that the mono-

Abbreviations: CKD=chronic kidney disease, DHE=dihydroethidium, FSC=forward-scatter, IS=indoxyl sulfate, Mac-1=macrophage 1 antigen, Nx=nephrectomized, SSC=side-scatter

1. Correspondence: Life Science and Bioethics, Dept. of International Health Development, Tokyo Medical and Dental University, Tokyo, 113-8510, Japan. E-mail: masa.vasc@tmd.ac.jp

cyte activation mediates vascular disease development in patients with renal injury.

AST-120 (Kremezin; Kureha, Tokyo, Japan) is known to retard the progression of CKD in humans and experimental animals by decreasing serum concentration of uremic toxins, such as IS [16–20]. IS is synthesized in the liver from indole, which is a metabolite of dietary protein-derived tryptophan produced by the intestinal flora, such as *Escherichia coli* [21]. IS is normally excreted in urine; however, serum levels of IS are increased significantly in patients with CKD compared with those in healthy individuals because of declining renal clearance [22]. A number of studies have indicated that IS stimulates glomerular sclerosis and fibrosis by producing free radicals, increasing expression of TGF-β1, tissue inhibitor of metalloproteinase-1, and proα1(I)collagen [23], whereas the accumulation of IS promotes renal failure [24–26]. IS also increases oxygen consumption in rat and human tubular cells as a result of the production of ROS. In contrast, AST-120 prevents hypoxia and ameliorates renal injury [27]. Other studies have also shown that IS promotes aortic calcification and enhances aortic wall thickening [23]. Furthermore, IS impairs vascular endothelial dilation in patients with CKD by inhibiting viability and NO production in endothelial cells [19, 23, 28], and it stimulates the proliferation of vascular smooth muscle cells by inducing oxidative stress [29–31]. In addition, we showed previously that IS induces leukocyte–endothelial interactions through the up-regulation of vascular endothelial adhesion molecules, such as E-selectin, via JNK- and oxidative stress-dependent pathways [32]. Taken together, these data indicate that IS plays a crucial role in the dysfunction of vascular smooth muscle cells and endothelial cells in CKD patients. However, the effect of IS on leukocyte dysfunction, which contributes to the progression of atherosclerosis and is found frequently in patients with renal disease, has not been well documented.

Therefore, the present study was designed to test the hypothesis that IS can induce the expression of adhesion molecules, such as Mac-1, and increase production of ROS in monocytes. We report for the first time that AST-120 administration lowers IS levels and thereby, improves CKD-induced monocyte Mac-1 expression and ROS generation in a Nx mice model. Furthermore, as indicated by our in vitro studies, IS enhances monocyte adhesion to vascular endothelium by inducing Mac-1 expression and augmenting oxidative stress in monocytes. The underlying mechanisms seem to involve activation of p38 MAPK and NAD(P)H oxidase-dependent ROS production. In conclusion, our findings reveal a previously unrecognized molecular link between uremic toxins and cardiovascular diseases.

MATERIALS AND METHODS

IS, RPMI-1640 medium, Dulbecco's PBS, NAD(P)H oxidase inhibitor (apocynin), mitochondrial electron transport inhibitor (rotenone), xanthine oxidase inhibitor (allopurinol), and anti-β-actin antibody were obtained from Sigma-Aldrich (St. Louis, MO, USA). The p38 MAPK phosphorylation inhibitor (SB203580), JNK phosphorylation inhibitor (SP600125), and MEK1/2 inhibitor (U0126) were purchased from Calbiochem (San Diego, CA, USA). Alexa Fluor 488-labeled anti-mouse Mac-1 (CD11b) mAb was obtained from Serotec (Oxford, UK). PerCP/Cy5.5-labeled anti-mouse CD45 mAb, APC-labeled anti-mouse CD115 mAb, and a functional blocking mAb against human Mac-1 were obtained from BioLegend (San Diego, CA, USA). DHE was purchased from Molecular Probes (Eugene, OR, USA). Anti-human Mac-1 (CD18; clone 7A10) was a generous gift from The Scripps Research Institute (La Jolla, CA, USA). Antiphospho-ERK, antiphospho-p38 MAPK, and antiphospho JNK antibodies were purchased from Cell Signaling Technology (Beverly, MA, USA).

Plasma biochemistry

Plasma urea, total cholesterol, HDL cholesterol, and triglyceride measurements were performed using an automated biochemical analyzer (Spotchem SP-4410; Arkray, Kyoto, Japan). Plasma IS was identified by HPLC.

Surgical procedure

Renal failure was induced in 9-week-old male C57BL/6J mice (Oriental Yeast, Tokyo, Japan) using a two-step surgical nephrectomy protocol, as described previously [32]. Briefly, under i.p. anesthesia induced by sodium pentobarbital (Schering-Plough, Kenilworth, NJ, USA) at 65 mg/kg, two of the three branches of the left renal artery were ligated through a lateral incision. One week after the first operation, the right kidney was removed after ligation of the renal blood vessels and ureter under anesthesia as described above. Four weeks after the procedure, blood pressure was measured by the tail-cuff method, and blood urea nitrogen was determined by an automated biochemical analyzer as described previously in Materials and Methods. Mice were allocated to experimental groups: one-half of the mice was fed a standard mouse diet containing 5% (w/v) of AST-120 (Nx+AST group; n=9), whereas the remaining mice were fed a regular diet (Nx; n=10) for 4 weeks. Sham-operated mice (n=10) received a regular diet and were used as the control group.

In another experiment, 10-week-old male C57BL/6J mice were administered 0.1% IS (200 mg/kg/day) in drinking water (n=10), whereas age-matched mice were given water alone (normal; n=10) and used as control animals. Four weeks after administration, these mice were killed, and whole blood samples were collected from the heart using heparinized syringes.

Flow cytometry analysis

Whole blood was lysed and incubated with Alexa Fluor 488-labeled anti-mouse Mac-1 mAb, PerCP/Cy5.5-labeled anti-mouse CD45 mAb, and APC-labeled anti-mouse CD115 mAb for 20 min, followed by incubation with DHE at 37°C for 25 min. Analysis of stained cells was performed using flow cytometry (FACSCalibur; BD Biosciences, San Jose, CA, USA), and the data were analyzed with FlowJo software (Treestar, San Carlos, CA, USA).

THP-1 cells were incubated with anti-human Mac-1 antibody, followed by incubation with Alexa Fluor 488-conjugated goat anti-mouse antibody. DHE was used to detect ROS generation. Fluorescence intensity was analyzed using flow cytometry as described above.

Cell culture

THP-1 cells, a human monocytic cell line, were obtained from the American Type Culture Collection (Manassas, VA, USA), and the cells were maintained in RPMI-1640 medium, supplemented with 10% FCS, 100 IU/mL penicillin, 100 μg/mL streptomycin, and 2 mmol/L L-glutamine in humidified 95% air with 5% CO_2 at 37°C. HUVECs were purchased from Sanko Junyaku (Tokyo, Japan). For use in the flow-chamber apparatus, HUVECs were placed onto 22-mm, fibronectin-coated glass coverslips.

Leukocyte adhesion assay

The protocols for an in vitro adhesion assay that mimics physiological flow conditions have been described in detail previously [32]. Briefly, HUVEC monolayers were stimulated with 10 U/mL IL-1β for 4 h on coverslips and then positioned in a flow chamber mounted on an inverted microscope (Nikon, Tokyo, Japan). THP-1 cells (1×10^6/mL) were incubated in 0, 0.2, 0.5, or 1.0 mmol/L IS for 1 h. For inhibitor treatment, all inhibitors were added 30 min before IS stimulation. After resuspending the cells in perfusion medium (PBS containing 0.2% human serum albumin), the cells were perfused through the chamber with a syringe pump (PHD2000; Harvard Apparatus, Holliston, MA, USA) for 10 min at a controlled flow rate to generate a shear stress of 1 dyne/cm^2. The entire period of perfusion was recorded by videotape and then analyzed by using image analysis software (Image Tracker PTV; Digimo, Osaka, Japan) to determine the number of rolling and adherent cells on HUVEC monolayers in 10 randomly selected, 15× (magnification) microscope fields.

Immunoblotting

Total cell lysates and membrane fraction of THP-1 cells (1×10^6/condition) were prepared as described previously [32]. Western blotting analysis was carried out with antibodies (described previously in Materials and Methods) using ECL Plus reagents (Amersham Pharmacia Biotech, Buckinghamshire, UK).

Statistical analysis

Results are expressed as mean ± SEM. Data were analyzed using one-way ANOVA with Tukey's post hoc analysis or a two-way ANOVA with the Bonferroni correction. P values <0.05 were considered statistically significant.

RESULTS

AST-120 attenuates CKD-induced Mac-1 expression and ROS production in vivo

To examine the effect of AST-120 on monocyte activation in vivo, we generated Nx CKD model mice and allocated them to AST-120-treated (Nx+AST; n=9) or untreated (Nx; n=10) groups. In Nx and Nx + AST groups, the systolic blood pressure, plasma urea, total cholesterol, HDL cholesterol, and triglyceride levels were elevated, and the body weight was low compared with that of sham-operated control mice (**Table 1**).

TABLE 1. Comparison among Sham, Nx, and Nx with AST-120 (Nx+AST) Mice

Parameter	Sham	Nx	Nx + AST
B.W. (g)	29.1 ± 1.9	28.1 ± 1.5[a]	28.2 ± 1.7[a]
Systolic BP (mmHg)	92 ± 9	119 ± 9[a]	117 ± 5[a]
Urea (mg/dL)	41 ± 5	72 ± 11[b]	77 ± 12[b]
Total cholesterol (mg/dL)	92 ± 14	111 ± 10[c]	109 ± 9[c]
HDL cholesterol (mg/dL)	55 ± 9	69 ± 5[b]	69 ± 7[b]
Triglyceride (mg/dL)	121 ± 26	152 ± 27[a]	153 ± 15[c]
White blood cells (10^2 cells/ul)	75 ± 16	77 ± 17	76 ± 21
IS (mg/dL)	0.31 ± 0.11	0.65 ± 0.21[b]	0.44 ± 0.17[d]

Data are means ± SD. B.W., Body weight; BP, blood pressure. [a]$P<0.05$ versus sham; [b]$P<0.001$ versus sham; [c]$P<0.01$ versus sham; [d]$P<0.05$ versus Nx.

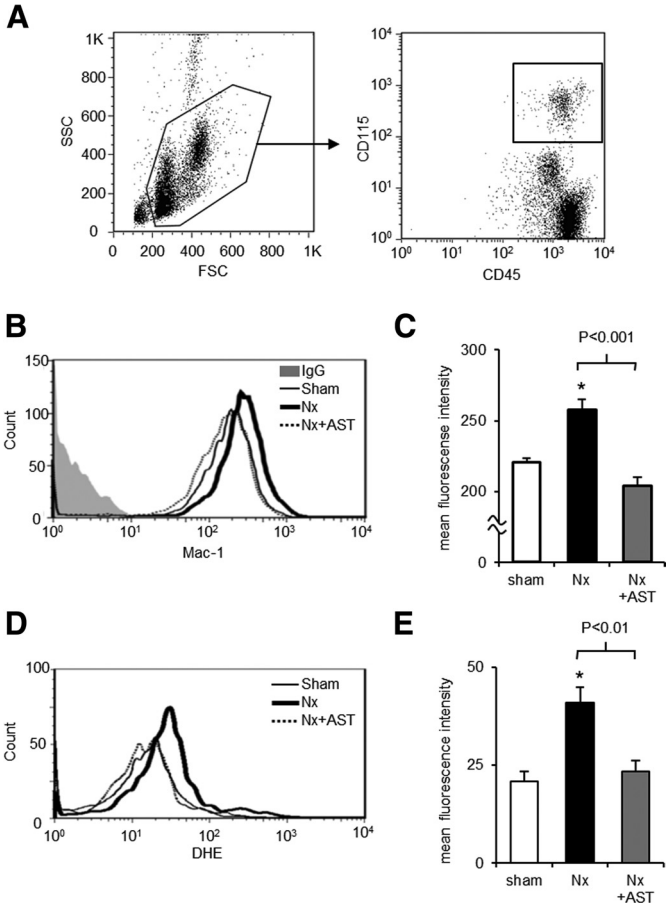

Figure 1. Effect of AST-120 on CKD-related monocyte-mediated inflammation. (A) Determination of peripheral blood monocytes. Cellular debris was excluded based on the FSC and SSC plots (gated area in the left panel). The double-positive cells that stained for CD45 and CD115 were identified as monocytes (gated area in right panel). Representative examples of peripheral blood monocytes stained with anti-Mac-1 antibody (B) and DHE to detect ROS production (D), detected by flow cytometry in Nx mice treated with (Nx+AST; dotted line) or without AST-120 (Nx; thick line) and in sham-operated mice (sham; thin line). An isotype control antibody was used as the negative control (gray filled). Quantitative analysis of Mac-1 expression (C) and ROS generation (E). White bars represent the sham-operated group (n=10), black bars represent the Nx group (n=10), and gray bars are Nx + AST group (n=9). Data are expressed as mean ± SEM. *$P<0.01$ versus sham, one-way ANOVA test with Tukey's post hoc analysis.

As expected, administration of AST-120 resulted in a significant reduction of plasma IS compared with that in the Nx group, whereas other plasma parameters, body weight, blood pressure, and number of white blood cells in the peripheral blood were not significantly different between Nx and Nx + AST groups (Table 1). The monocyte population was determined based on double-positive staining for CD45 and CD115 after excluding cellular debris and doublets by gating based on the FSC and SSC properties, as shown in **Fig. 1A**. Flow cytometry analysis of peripheral blood monocytes showed that Mac-1 expression and ROS production

were increased significantly in the Nx group compared with that of the sham group. AST-120 therapy improved CKD-enhanced Mac-1 expression and ROS production in monocytes (Fig. 1). However, the expression level of Mac-1 in granulocytes was not significantly different between sham and Nx groups (data not shown).

IS directly enhanced monocyte-mediated inflammation in vivo

To further elucidate the importance of IS in monocyte-mediated inflammation, we performed flow cytometry on peripheral blood monocytes obtained from mice that received IS in drinking water or only water (normal) for 4 weeks. Plasma IS was significantly elevated in the IS group, whereas other parameters, such as urea, lipids, and body weight, were not significantly different between the IS and normal groups (**Table 2**). Flow cytometry analysis of peripheral blood monocytes revealed significant activation of Mac-1 and ROS production in mice that received drinking water with IS compared with that in normal mice (**Fig. 2**).

IS induced monocyte adhesion to vascular endothelium in vitro

First, we examined the effects of IS on monocyte–endothelial interactions under physiological flow conditions (shear stress, 1 dyne/cm^2) in vitro. Treatment of THP-1 cells with 1 mmol/L IS for 1 h significantly induced adhesion to 10 U/mL IL-1β-stimulated HUVECs (**Fig. 3A**), whereas treatment with IS for 0.5, 4, or 24 h did not enhance THP-1 cell adhesion to HUVECs (Fig. 3B). IS also enhanced THP-1 cell adhesion in a dose-dependent manner (Fig. 3C). Based on these results, we incubated THP-1 cells with IS (1.0 mmol/L) for 1 h in subsequent cell adhesion assays.

As integrin expression on monocytes plays a crucial role in adhesion of monocytes to vascular endothelial cells, we examined Mac-1 expression in THP-1 cells treated with IS by using flow cytometry. As shown in Fig. 3D and E, treatment with IS for 1 h dose-dependently enhanced Mac-1 expression in THP-1 cells.

Furthermore, a functional blocking antibody for Mac-1 significantly reduced THP-1 cell adhesion to HUVECs (Fig. 3F).

TABLE 2. Comparison between Normal and IS-Treated Mice

Parameter	Normal	IS
B.W. (g)	29.1 ± 1.9	28.1 ± 1.5
Systolic BP (mmHg)	109 ± 5	107 ± 7
Urea (mg/dL)	33 ± 3	35 ± 3
Total cholesterol (mg/dL)	100 ± 11	99 ± 9
HDL cholesterol (mg/dL)	59 ± 7	57 ± 6
Triglyceride (mg/dL)	129 ± 17	147 ± 29
White blood cells (10^2 cells/ul)	76 ± 22	77 ± 20
IS (mg/dL)	0.33 ± 0.15	0.94 ± 0.23[a]

Data are means ± SD. [a]$P < 0.0001$ versus normal.

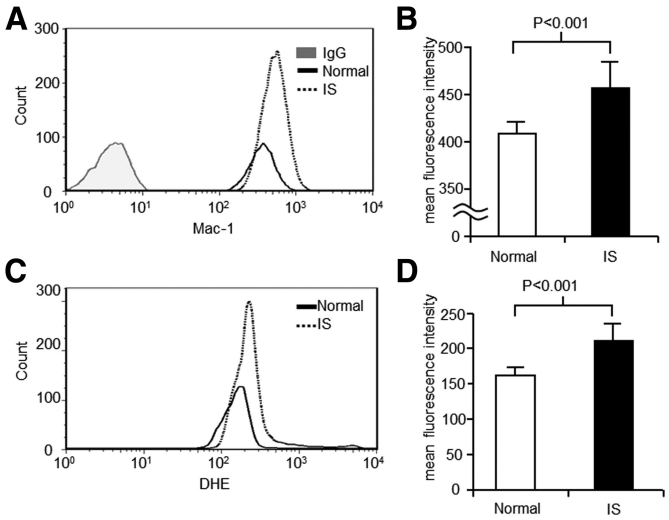

Figure 2. Effect of IS on monocyte-mediated inflammation in vivo. Representative examples of peripheral blood monocyte staining using flow cytometry to analyze the expression of Mac-1 (A) and ROS production detected by DHE (C) in mice treated with (IS; dotted) or without IS (Normal; line). An isotype control antibody was used as a negative control (gray, filled). Quantitative analysis of Mac-1 expression (B) and ROS generation (D). White bars represent normal mice group, whereas black bars represent IS group. Data are expressed as mean ± SEM (n=10). Statistical analysis was performed using one-way ANOVA test with Tukey's post hoc analysis.

p38 MAPK signaling pathway involved in monocyte activation

To further elucidate the molecular mechanisms involved in IS-mediated monocyte activation, we examined the role of MAPK family members p38 MAPK, JNK, and ERK1/2. Western blot analyses revealed that IS enhanced phosphorylation of p38 MAPK but did not enhance phosphorylation of JNK or ERK1/2 in THP-1 cells (**Fig. 4A**). To further determine the role of p38 MAPK, we examined the effect of inhibitors of the MAPK pathways, such as p38 MAPK, JNK, and ERK1/2. Although all inhibitors reduced baseline THP-1 adhesion, only SB203580, a chemical inhibitor of p38 MAPK signaling pathway, abrogated the IS-induced enhancement of THP-1 cell adhesion to HUVECs at baseline, whereas the JNK inhibitor SP600125 and the ERK1/2 inhibitor U0126 did not inhibit THP-1 cell adhesion at baseline (Fig. 4B). Moreover, SB203580 suppressed IS-induced Mac-1 expression (Fig. 4C). In contrast, neither SP600125 (Fig. 4D) nor U0126 (Fig. 4E) altered IS-enhanced Mac-1 expression (Fig. 4F).

Role of oxidative stress in monocytic cell adhesion and Mac-1 expression

As IS has been shown to cause oxidative stress in various cells [29–32], we evaluated the role of intracellular ROS in IS-mediated monocyte activation. Staining for ROS estimation was performed using DHE, followed by flow cytometric analysis, which showed that IS dose-dependently induced ROS production in THP-1 cells (**Fig. 5A** and **B**). To identify the mechanisms underlying the oxidative stress caused by IS, we tested whether

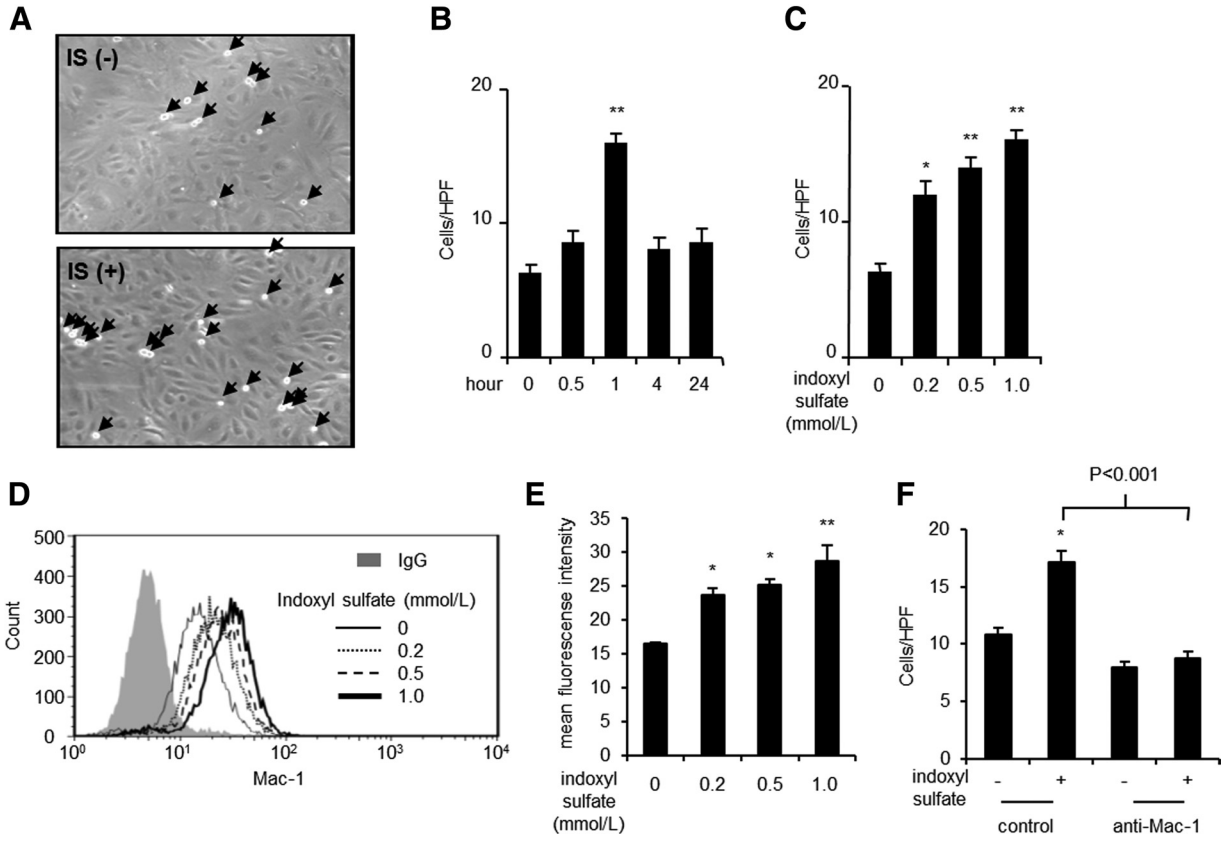

Figure 3. Effect of IS on monocyte-mediated inflammation in vitro. Representative phase contrast micrographs showing adhesion of THP-1 cells stimulated with (IS+) and without (IS−) IS (1 mmol/L for 1 h) to 10 U/mL IL-1β-activated HUVECs. Arrowheads indicate adhered THP-1 cells. Original magnification, 200×. Adhesion assay in THP-1 cells (1×10^6 cells/mL in 12-well plate) treated with 1 mmol/L IS for 0, 0.5, 1, 4, 24 h (B) or stimulated with indicated concentrations of IS for 1 h (C). Adhesion assay data are shown as mean ± SEM (n=10). *$P < 0.01$; **$P < 0.001$ versus nontreated THP-1 cells, one-way ANOVA test with Tukey's post hoc analysis. HPF, High-power field. (D) Flow cytometric analysis of Mac-1 expression in THP-1 cells treated with 0 (thin line), 0.2 (dotted line), 0.5 (dashed line), and 1.0 (thick line) mmol/L IS for 1 h. An isotype control antibody was used as a negative control. (E) Quantitative analysis of Mac-1 expression in THP-1 cells treated with 0, 0.2, 0.5, and 1 mmol/L IS for 1 h. *$P < 0.01$; **$P < 0.001$ versus nontreated THP-1 cells, one-way ANOVA test with Tukey's post hoc analysis. (F) Adhesion assay in THP-1 cells (1×10^6 cells/mL in 12-well plate) treated with anti-Mac-1 mAb or control IgG (20 μg/mL), followed by addition of 1 mmol/L IS for 1 h. *$P < 0.001$ versus control antibody-treated THP-1 cells. Results are expressed as mean ± SEM. Statistical analysis was performed using a two-way ANOVA with the Bonferroni correction. These data are representative of three independent experiments.

NAD(P)H oxidase activation was crucial to monocyte activation. Western blot analysis revealed that membrane translocation of NAD(P)H oxidase subunit p47phox was increased and peaked at 30 min after treatment with IS and decreased thereafter (Fig. 5C, upper panels). IS also enhanced membrane translocation of p47 phox in a dose-dependent manner (Fig. 5C, lower panels). The NAD(P)H oxidase inhibitor apocynin reduced IS-induced THP-1 cell adhesion to HUVECs (Fig. 5D). In contrast to apocynin, rotenone (inhibitor of mitochondrial electron transport) and allopurinol (xanthine oxidase inhibitor) failed to change IS-induced THP-1 cell adhesion (Fig. 5D). Apocynin also suppressed Mac-1 expression and ROS production in THP-1 cells (Fig. 5D and E). Neither rotenone nor allopurinol suppressed IS-induced Mac-1 expression and ROS production (data not shown).

DISCUSSION

Our main finding was that AST-120 ameliorated CKD-induced Mac-1 expression and ROS production by the reduction of IS. AST-120 prevents the aggravation of fibrosis in kidney and heart by reducing oxidative stress in experimental animal models [23, 33–35]. However, the precise mechanisms have not been clearly identified.

Oxidative stress is involved in the progression of renal damage in patients with diabetic nephropathy [36] and is correlated significantly with glomerular abnormalities in diabetic nephropathy [37]. Furthermore, monocytes/macrophages have been shown to accumulate in the extracapillary areas of glomeruli [38, 39]. In addition, reduction of oxidative stress has been shown to reduce macrophage infiltration and improve renal function [40]. Thus, these observa-

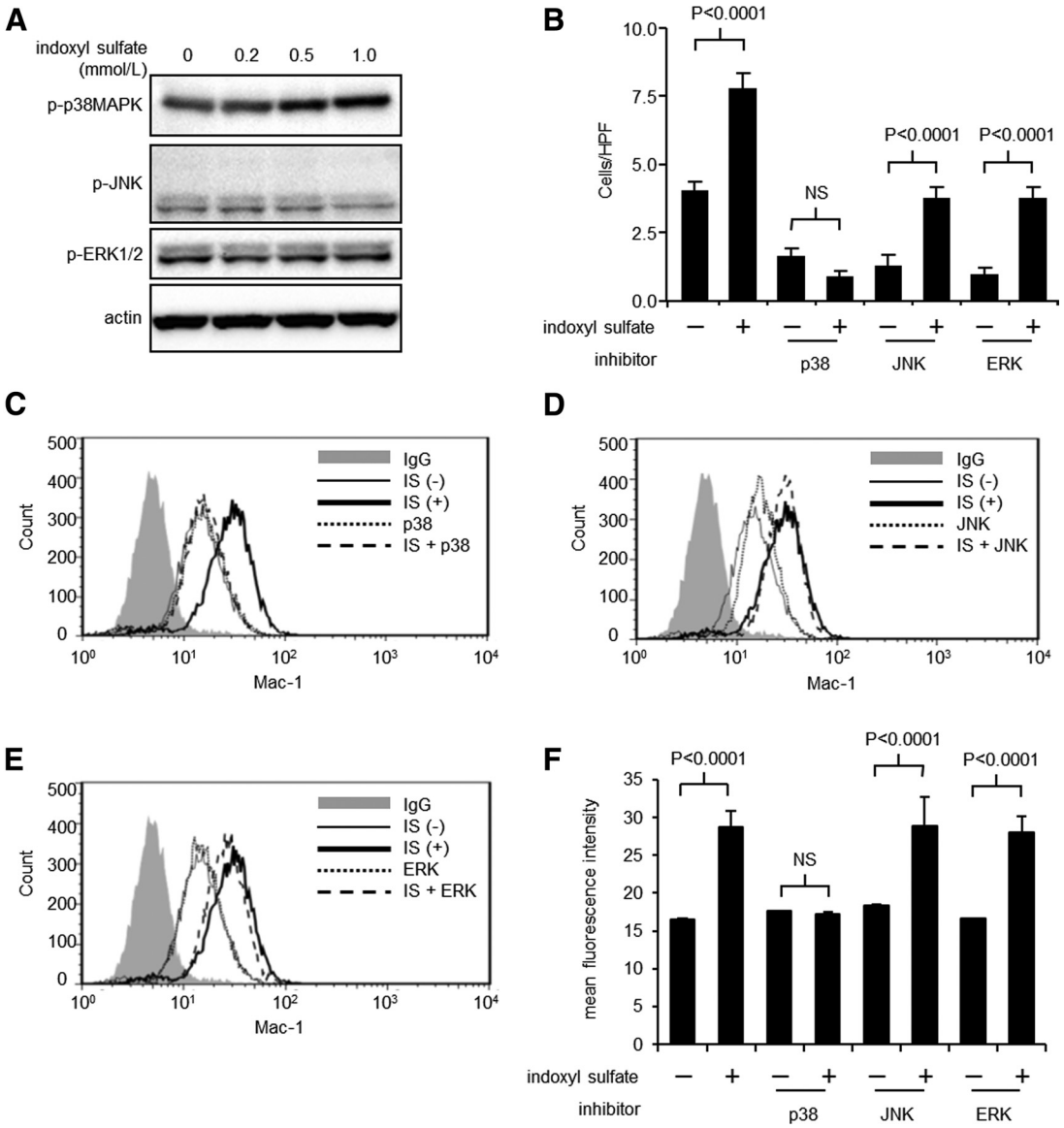

Figure 4. Effect of IS on the p38 MAPK pathway. Western blot detection of phosphorylated MAPK family members p38 MAPK, JNK, and ERK1/2. THP-1 cells (1×10^6 cells/mL in 12-well plate) were incubated in the presence of the indicated concentrations of IS for 1 h. Adhesion assay in THP-1 cells treated with the p38 MAPK inhibitor SB203580 (p38: 5 μmol/L), JNK inhibitor SP600125 (JNK: 10 μmol/L), or ERK1/2 inhibitor U0126 (ERK: 10 μmol/L) for 30 min, followed by incubation with (+) or without (−) 1 mmol/L IS for 1 h. The cells were then subjected to adhesion assays. Data of adhesion assay are shown as mean ± SEM (n=10). Statistical analysis was performed using a two-way ANOVA with the Bonferroni correction. Flow cytometric analysis of THP-1 cells stained with anti-Mac-1 antibody in THP-1 cells treated with p38 MAPK inhibitor SB203580 (p38: 5 μmol/L; C), JNK inhibitor SP600125 (JNK: 10 μmol/L; D), or ERK inhibitor U0126 (ERK: 10 μmol/L; E), followed by stimulation with 1 mmol/L IS for 1 h. The data shown are representative of three independent experiments. (F) Quantitative analysis of Mac-1 expression in THP-1 cells performed by flow cytometry in C–E. Statistical analysis was performed using a two-way ANOVA with the Bonferroni correction.

tions suggest that ROS and monocyte activation also play an important role in the pathogenesis of renal dysfunction.

Our group reported previously that inhibition of NAD(P)H oxidase in leukocytes dramatically decreased leukocyte–endothelial interaction in a wire-injured vascular inflammation model [41], and Mac-1 deficiency ameliorated vascular injury [10, 11], indicating that Mac-1 and oxidative burst in leukocytes play an important role in atherosclerosis development. In fact, IS-induced THP-1 adhesion was blocked by an anti-Mac-1 antibody and inhibitor of NAD(P)H oxidase.

These observations also suggest that kidney injury and atherosclerosis have a common pathway in terms of oxidative stress and infiltration of monocytes/macrophages. Palm et al. [27] clearly demonstrated that IS-lowering therapy by AST-120 administration decreased tubule-intestinal macro-

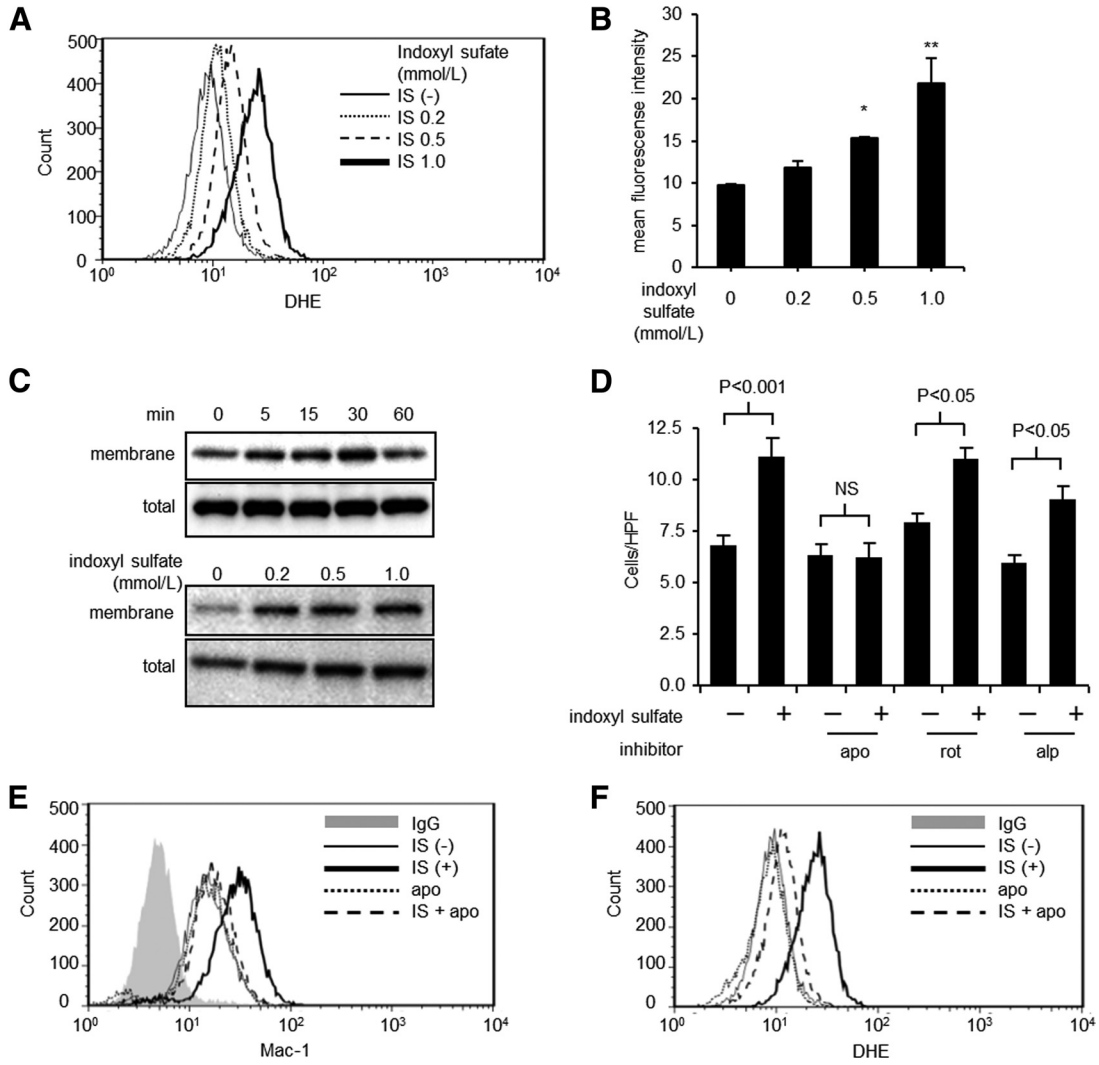

Figure 5. Effect of IS on NAD(P)H oxidase-dependent ROS production. Flow cytometry analysis of THP-1 cells (1×10^6 cells/mL in 12-well plate) treated with 0 (thin line), 0.2 (dotted line), 0.5 (dashed line), and 1.0 (thick line) mmol/L IS, followed by staining with DHE to detect ROS generation. (B) Quantitative analysis of Mac-1 expression in THP-1 cells treated with 0, 0.2, 0.5, and 1.0 mmol/L IS for 1 h. $*P < 0.01$; $**P < 0.001$ versus nontreated THP-1 cells, one-way ANOVA test with Tukey's post hoc analysis. (C) Western blot detection of NAD(P)H oxidase subunit p47phox in membrane fraction and the total cell homogenates. THP-1 cells (1×10^6 cells/mL in 12-well plate) were incubated in the presence of 1 mmol/L IS for the indicated period (upper panels) or treated with indicated concentrations of IS for 30 min (lower panels). (D) THP-1 cells (1×10^6 cells/mL in 12-well plate) were treated with the NAD(P)H oxidase inhibitor, apocynin (apo; 200 μmol/L); mitochondrial electron transport inhibitor, rotenone (rot; 5 μmol/L); or xanthine oxidase inhibitor, allopurinol (alp; 100 μmol/L) for 30 min, followed by incubation with (+) or without (−) 1 mmol/L IS for 1 h; the cells were subjected to adhesion assays. Data of adhesion assay are mean ± SEM (n=10). Statistical analysis was performed using a two-way ANOVA with the Bonferroni correction. Flow cytometric analysis of THP-1 cells stained with anti-Mac-1 antibody (E) and DHE (F). Cells were treated with apocynin for 30 min, followed by stimulation with 1 mmol/L IS for 1 h. The data shown are representative of three independent experiments.

phage influx by reducing oxidative stress. Our results may link the mechanisms that enable AST-120 in diminishing infiltration of monocytes/macrophages to the kidney. Furthermore, our data partly explain a recent report by Barreto et al. [42], which shows an association of serum IS with the incidence of cardiovascular diseases and total mortality in CKD patients.

Previously, we showed that IS induced oxidative stress in vascular endothelium. Numerous factors, such as the rennin-angiotensin system, hypertension, infection, and antioxidant deficiency, appear to be involved in oxidative stress and inflammation in CKD [12]. Our results indicated that oxidative stress in leukocytes is partially a result of the accumulation of uremic toxins, such as IS, in patients with renal disease. AST-120 also decreased various types of uremic toxins in serum, such as hippuric acid, phenyl sulfate, and 4-ethylphenyl sulfate [20], suggesting a critical role for uremic toxin in the activation of monocytes in vivo. Other uremic toxins may also be potentially involved with CKD-related oxidative stress.

We showed previously that IS enhanced p38 MAPK and JNK in vascular endothelial cells, suggesting that distinct signaling pathways were involved in monocytes. An inhibitor of p38 MAPK did not suppress IS-induced oxidative stress (data not shown). Furthermore, NAD(P)H oxidase activated p38MAPK, which mediated Mac-1 expression induced by ischemia-reperfusion injury [43, 44] and by proinflammatory cytokines, such as TNF-α [45]. These observations strongly suggested that p38 MAPK was downstream of ROS and upstream of Mac-1.

As shown in Fig. 3B, induction of IS on THP-1 adhesion peaked after 1-h incubation. This pattern is in contrast to effect of IS on HUVECs, where IS-dependent adhesion was maximum after 4 h of incubation with TNF-α. This difference may have resulted from distinct intracellular machinery in monocytes and HUVECs.

In conclusion, IS directly induced cell-surface expression of Mac-1 and increased oxidative stress in vitro and in vivo. Notably, AST-120 administration attenuated monocyte activation in vivo. In addition, IS-enhanced monocyte activation may be mediated by activation of p38 MAPK- and NAD(P)H oxidase-dependent pathways. Thus, our data suggest a novel role for uremic toxins that enables the toxins to produce vascular inflammation in patients with renal dysfunction.

AUTHORSHIP

S.I. performed experiments, analyzed the data, and wrote the paper. Y.H. and Y.Y. performed the research. F.N. and H.Y. designed the research and analyzed the data. M.O., H.I., and M.Y. designed the research, analyzed the data, and wrote the paper.

ACKNOWLEDGMENTS

We gratefully acknowledge the expert assistance of Daisuke Mori, Nana Yamamoto, and Toshie Kaizuka for working with the cell cultures. We thank Minako Manabe and Kazumi Obara for assistance with HPLC analyses. We also thank Yusuke Yamashita for technical assistance with animal surgery.

REFERENCES

1. Wheeler, D. C. (1996) Cardiovascular disease in patients with chronic renal failure. *Lancet* **348,** 1673–1674.
2. Amann, K., Gross, M. L., Ritz, E. (2004) Pathophysiology underlying accelerated atherogenesis in renal disease: closing in on the target. *J. Am. Soc. Nephrol.* **15,** 1664–1666.
3. Go, A. S., Chertow, G. M., Fan, D., McCulloch, C. E., Hsu, C. Y. (2004) Chronic kidney disease and the risks of death, cardiovascular events, and hospitalization. *N. Engl. J. Med.* **351,** 1296–1305.
4. Ronco, C., Haapio, M., House, A. A., Anavekar, N., Bellomo, R. (2008) Cardiorenal syndrome. *J. Am. Coll. Cardiol.* **52,** 1527–1539.
5. Ross, R. (1999) Atherosclerosis—an inflammatory disease. *N. Engl. J. Med.* **340,** 115–126.
6. Pietersma, A., Kofflard, M., de Wit, L. E., Stijnen, T., Koster, J. F., Serruys, P. W., Sluiter, W. (1995) Late lumen loss after coronary angioplasty is associated with the activation status of circulating phagocytes before treatment. *Circulation* **91,** 1320–1325.
7. Nageh, M. F., Sandberg, E. T., Marotti, K. R., Lin, A. H., Melchior, E. P., Bullard, D. C., Beaudet, A. L. (1997) Deficiency of inflammatory cell adhesion molecules protects against atherosclerosis in mice. *Arterioscler. Thromb. Vasc. Biol.* **17,** 1517–1520.
8. Hynes, R. O. (1987) Integrins: a family of cell surface receptors. *Cell* **48,** 549–554.
9. Hynes, R. O. (1992) Integrins: versatility, modulation, and signaling in cell adhesion. *Cell* **69,** 11–25.
10. Rogers, C., Edelman, E. R., Simon, D. I. (1998) A mAb to the β2-leukocyte integrin Mac-1 (CD11b/CD18) reduces intimal thickening after angioplasty or stent implantation in rabbits. *Proc. Natl. Acad. Sci. USA* **95,** 10134–10139.
11. Simon, D. I., Dhen, Z., Seifert, P., Edelman, E. R., Ballantyne, C. M., Rogers, C. (2000) Decreased neointimal formation in Mac-1(−/−) mice reveals a role for inflammation in vascular repair after angioplasty. *J. Clin. Invest.* **105,** 293–300.
12. Yoon, J. W., Pahl, M. V., Vaziri, N. D. (2007) Spontaneous leukocyte activation and oxygen-free radical generation in end-stage renal disease. *Kidney Int.* **71,** 167–172.
13. Stenvinkel, P., Ketteler, M., Johnson, R. J., Lindholm, B., Pecoits-Filho, R., Riella, M., Heimburger, O., Cederholm, T., Girndt, M. (2005) IL-10, IL-6, and TNF-α: central factors in the altered cytokine network of uremia—the good, the bad, and the ugly. *Kidney Int.* **67,** 1216–1233.
14. Anrather, J., Racchumi, G., Iadecola, C. (2006) NF-κB regulates phagocytic NADPH oxidase by inducing the expression of gp91phox. *J. Biol. Chem.* **281,** 5657–5667.
15. Kaul, N., Devaraj, S., Jialal, I. (2001) α-Tocopherol and atherosclerosis. *Exp. Biol. Med. (Maywood)* **226,** 5–12.
16. Schulman, G., Agarwal, R., Acharya, M., Berl, T., Blumenthal, S., Kopyt, N. (2006) A multicenter, randomized, double-blind, placebo-controlled, dose-ranging study of AST-120 (Kremezin) in patients with moderate to severe CKD. *Am. J. Kidney Dis.* **47,** 565–577.
17. Iida, S., Kohno, K., Yoshimura, J., Ueda, S., Usui, M., Miyazaki, H., Nishida, H., Tamaki, K., Okuda, S. (2006) Carbonic-adsorbent AST-120 reduces overload of IS and the plasma level of TGF-β1 in patients with chronic renal failure. *Clin. Exp. Nephrol.* **10,** 262–267.
18. Shoji, T., Wada, A., Inoue, K., Hayashi, D., Tomida, K., Furumatsu, Y., Kaneko, T., Okada, N., Fukuhara, Y., Imai, E., Tsubakihara, Y. (2007) Prospective randomized study evaluating the efficacy of the spherical adsorptive carbon AST-120 in chronic kidney disease patients with moderate decrease in renal function. *Nephron. Clin. Pract.* **105,** c99–c107.
19. Namikoshi, T., Tomita, N., Satoh, M., Sakuta, T., Kuwabara, A., Kobayashi, S., Higuchi, Y., Nishijima, F., Kashihara, N. (2009) Oral adsorbent AST-120 ameliorates endothelial dysfunction independent of renal function in rats with subtotal nephrectomy. *Hypertens. Res.* **32,** 194–200.
20. Kikuchi, K., Itoh, Y., Tateoka, R., Ezawa, A., Murakami, K., Niwa, T. (2010) Metabolomic search for uremic toxins as indicators of the effect of an oral sorbent AST-120 by liquid chromatography/tandem mass spectrometry. *J. Chromatogr. B Analyt. Technol. Biomed. Life Sci.* **878,** 2997–3002.
21. Vanholder, R., De Smet, R. (1999) Pathophysiologic effects of uremic retention solutes. *J. Am. Soc. Nephrol.* **10,** 1815–1823.
22. Vanholder, R., De Smet, R., Glorieux, G., Argiles, A., Baurmeister, U., Brunet, P., Clark, W., Cohen, G., De Deyn, P. P., Deppisch, R., Descamps-Latscha, B., Henle, T., Jorres, A., Lemke, H. D., Massy, Z. A., Passlick-Deetjen, J., Rodriguez, M., Stegmayr, B., Stenvinkel, P., Tetta, C., Wanner, C., Zidek, W. (2003) Review on uremic toxins: classification, concentration, and interindividual variability. *Kidney Int.* **63,** 1934–1943.
23. Niwa, T. (2010) Indoxyl sulfate is a nephro-vascular toxin. *J. Ren. Nutr.* **20,** S2–S6.
24. Niwa, T., Ise, M. (1994) Indoxyl sulfate, a circulating uremic toxin, stimulates the progression of glomerular sclerosis. *J. Lab. Clin. Med.* **124,** 96–104.
25. Niwa, T., Ise, M., Miyazaki, T. (1994) Progression of glomerular sclerosis in experimental uremic rats by administration of indole, a precursor of indoxyl sulfate. *Am. J. Nephrol.* **14,** 207–212.
26. Kobayashi, N., Maeda, A., Horikoshi, S., Shirato, I., Tomino, Y., Ise, M. (2002) Effects of oral adsorbent AST-120 (Kremezin) on renal function and glomerular injury in early-stage renal failure of subtotal nephrectomized rats. *Nephron* **91,** 480–485.
27. Palm, F., Nangaku, M., Fasching, A., Tanaka, T., Nordquist, L., Hansell, P., Kawakami, T., Nishijima, F., Fujita, T. (2010) Uremia induces abnormal oxygen consumption in tubules and aggravates chronic hypoxia of the kidney via oxidative stress. *Am. J. Physiol. Renal Physiol.* **299,** F380–F386.
28. Yu, M., Kim, Y. J., Kang, D. H. (2011) Indoxyl sulfate-induced endothelial dysfunction in patients with chronic kidney disease via an induction of oxidative stress. *Clin. J. Am. Soc. Nephrol.* **6,** 30–39.
29. Yamamoto, H., Tsuruoka, S., Ioka, T., Ando, H., Ito, C., Akimoto, T., Fujimura, A., Asano, Y., Kusano, E. (2006) Indoxyl sulfate stimulates proliferation of rat vascular smooth muscle cells. *Kidney Int.* **69,** 1780–1785.
30. Shimizu, H., Hirose, Y., Nishijima, F., Tsubakihara, Y., Miyazaki, H. (2009) ROS and PDGF-β [corrected] receptors are critically involved in

indoxyl sulfate actions that promote vascular smooth muscle cell proliferation and migration. *Am. J. Physiol. Cell. Physiol.* **297,** C389–C396.
31. Muteliefu, G., Enomoto, A., Niwa, T. (2009) Indoxyl sulfate promotes proliferation of human aortic smooth muscle cells by inducing oxidative stress. *J. Ren. Nutr.* **19,** 29–32.
32. Ito, S., Osaka, M., Higuchi, Y., Nishijima, F., Ishii, H., Yoshida, M. (2010) Indoxyl sulfate induces leukocyte-endothelial interactions through up-regulation of E-selectin. *J. Biol. Chem.* **285,** 38869–38875.
33. Nakai, K., Fujii, H., Kono, K., Goto, S., Fukagawa, M., Nishi, S. (2011) Effects of AST-120 on left ventricular mass in predialysis patients. *Am. J. Nephrol.* **33,** 218–223.
34. Shibahara, H., Shibahara, N. (2010) Cardiorenal protective effect of the oral uremic toxin absorbent AST-120 in chronic heart disease patients with moderate CKD. *J. Nephrol.* **23,** 535–540.
35. Fujii, H., Nishijima, F., Goto, S., Sugano, M., Yamato, H., Kitazawa, R., Kitazawa, S., Fukagawa, M. (2009) Oral charcoal adsorbent (AST-120) prevents progression of cardiac damage in chronic kidney disease through suppression of oxidative stress. *Nephrol. Dial. Transplant.* **24,** 2089–2095.
36. Prabhakar, S., Starnes, J., Shi, S., Lonis, B., Tran, R. (2007) Diabetic nephropathy is associated with oxidative stress and decreased renal nitric oxide production. *J. Am. Soc. Nephrol.* **18,** 2945–2952.
37. Fujii, H., Kono, K., Nakai, K., Goto, S., Komaba, H., Hamada, Y., Shinohara, M., Kitazawa, R., Kitazawa, S., Fukagawa, M. (2010) Oxidative and nitrosative stress and progression of diabetic nephropathy in type 2 diabetes. *Am. J. Nephrol.* **31,** 342–352.
38. Bolton, W. K., Innes D. J., Jr., Sturgill, B. C., Kaiser, D. L. (1987) T-cells and macrophages in rapidly progressive glomerulonephritis: clinicopathologic correlations. *Kidney Int.* **32,** 869–876.
39. Nakatani, K., Fujii, H., Hasegawa, H., Terada, M., Arita, N., Ito, M. R., Ono, M., Takahashi, S., Saiga, K., Yoshimoto, S., Iwano, M., Shiiki, H., Saito, Y., Nose, M. (2004) Endothelial adhesion molecules in glomerular lesions: association with their severity and diversity in lupus models. *Kidney Int.* **65,** 1290–1300.
40. Wu, Y. G., Lin, H., Qi, X. M., Wu, G. Z., Qian, H., Zhao, M., Shen, J. J., Lin, S. T. (2006) Prevention of early renal injury by mycophenolate mofetil and its mechanism in experimental diabetes. *Int. Immunopharmacol.* **6,** 445–453.
41. Hagita, S., Osaka, M., Shimokado, K., Yoshida, M. (2008) Oxidative stress in mononuclear cells plays a dominant role in their adhesion to mouse femoral artery after injury. *Hypertension* **51,** 797–802.
42. Barreto, F. C., Barreto, D. V., Liabeuf, S., Meert, N., Glorieux, G., Temmar, M., Choukroun, G., Vanholder, R., Massy, Z. A. (2009) Serum indoxyl sulfate is associated with vascular disease and mortality in chronic kidney disease patients. *Clin. J. Am. Soc. Nephrol.* **4,** 1551–1558.
43. Mendez-Samperio, P., Perez, A., Alba, L. (2010) Reactive oxygen species-activated p38/ERK 1/2 MAPK signaling pathway in the *Mycobacterium bovis* bacillus Calmette Guerin (BCG)-induced CCL2 secretion in human monocytic cell line THP-1. *Arch. Med. Res.* **41,** 579–585.
44. Ghori, K., O'Driscoll, J., Shorten, G. (2010) The effect of midazolam on neutrophil mitogen-activated protein kinase. *Eur. J. Anaesthesiol.* **27,** 562–565.
45. Lekawanvijit, S., Adrahtas, A., Kelly, D. J., Kompa, A. R., Wang, B. H., Krum, H. (2010) Does indoxyl sulfate, a uraemic toxin, have direct effects on cardiac fibroblasts and myocytes? *Eur. Heart. J.* **31,** 1771–1779.

KEY WORDS:
uremic toxin · atherosclerosis · leukocyte–endothelial interactions · adhesion molecule · oxidative stress